Structure and organization of nanosized-inclusion-containing bilayer membranes

Chun-lai Ren and Yu-qiang Ma*
National Laboratory of Solid State Microstructures, Nanjing University, Nanjing 210093, China
(Received 4 July 2006; revised manuscript received 11 May 2009; published 15 July 2009)

Based on a considerable amount of experimental evidence for lateral organization of lipid membranes which share astonishingly similar features in the presence of different inclusions, we use a hybrid self-consistent field theory (SCFT)/density-functional theory (DFT) approach to deal with bilayer membranes embedded by nanosized inclusions and explain experimental findings. Here, the hydrophobic inclusions are simple models of hydrophobic drugs or other nanoparticles for biomedical applications. It is found that lipid/inclusion-rich domains are formed at moderate inclusion concentrations and disappear with the increase in the concentration of inclusions. At high inclusion content, chaining of inclusions occurs due to the effective depletion attraction between inclusions mediated by lipids. Meanwhile, the increase in the concentration of inclusions can also cause thickening of the membrane and the distribution of inclusions undergoes a layering transition from one-layer structure located in the bilayer midplane to two-layer structure arranged into the two leaflets of a bilayer. Our theoretical predictions address the complex interactions between membranes and inclusions suggesting a unifying mechanism which reflects the competition between the conformational entropy of lipids favoring the formation of lipid- and inclusion-rich domains in lipids and the steric repulsion of inclusions leading to the uniform dispersion.

DOI: 10.1103/PhysRevE.80.011910 PACS number(s): 87.16.D−

I. INTRODUCTION

Membrane organization is essential for cellular functions such as signal transduction and membrane trafficking. A major challenge is to understand the lateral heterogeneous structures in membranes and membrane fluidity in the presence of inclusions. In recent years, there is growing evidence that due to the presence of inclusions within membranes, the distribution of lipids is inhomogeneous, where lateral segregation could induce the formation of lipid/inclusion-rich raft domains. For instance, cholesterol, which is one of the most important regulators of lipid organization, prefers to have conformationally ordered lipid chains next to it due to its hydrophobically smooth and stiff steroid ring structure [1,2] and promotes the formation of lipid rafts (see, for example, reviews [1,3–8] and recent research works [9–14]). On the other hand, it has been reported [15] that hydrophobic drugs such as taxol (paclitaxel) [15,16] and dipyridamole (DIP) [17] may assist the formation of lipid- and drug-enriched raft domains. This tendency increases with increasing the drug content, but disappears at high concentrations, a phenomenon which has also been observed in cholesterol-lipid systems [18]. Particularly, the perturbed lipids may produce the effective depletion attraction between inclusions leading to the chaining of cholesterols [18,19] or drugs [15,20] inside the bilayer. Such a lipid-mediated depletion attraction is also found in membrane-peptide systems [21,22]. Furthermore, the introducing of taxol drug into the lipid layer will perturb the hydrocarbon chain conformation, which may increase membrane fluidity [15,16,20]. Most recently, some foreign inclusions such as silver nanoparticles were reported to have similar effects on the membrane fluidity [23].

Despite the common properties of membrane organization due to distinct inclusions and despite its important significance in cellular functions such as signal transduction and membrane trafficking [3–7], the understanding of the mechanisms remains poor [24] due to the complexity of membrane/inclusion systems. Recently, some theoretical works have focused on the hydrophobic mismatch interaction between inclusions [25–29] and the possible formation of lipid rafts [1,24], which are very useful to raise our understanding. However, the lateral reorganization of lipid membranes with varying the inclusion content has not been systematically elucidated theoretically. To capture the lateral structure of inclusion-containing membranes, models must describe the membrane deformation in three dimensions. Due to the large computational consuming, it is convenient to use a coarse-grained model for the computational efficiency.

Recently, the self-consistent field theory (SCFT) has been proven to be powerful in calculating equilibrium morphologies in polymeric systems [30–37], while nanoparticles can be treated by density-functional theory (DFT) [38,39] to account for steric packing effects of particles. Interestingly, Thompson *et al.* [30] developed a hybrid SCFT/DFT approach to study mixtures of diblock copolymer and nanoparticles. On the other hand, the SCFT method is extended to successfully study the phase behavior of pure lipid systems [24,40–43]. Leermakers and co-workers [41–43] used a lattice version of SCFT to study the lipid-bilayer system, where the conformation of lipid chains is described by random-walk and rotational isomeric state (RIS) statistics. However, in most of their works, they assumed that the lipid bilayer was laterally homogeneous for computational convenience. On the contrary, Schick and co-workers [24] adopted the off-lattice version of SCFT to study the lipid systems, where they use Gaussian model to describe the lipid molecules. The amphiphilic nature and chain stretching of lipids are still captured. Compared to the lattice version of SCFT used by Leermakers and co-workers, the off-lattice SCFT can ac-

*Author to whom correspondence should be addressed; myqiang@nju.edu.cn

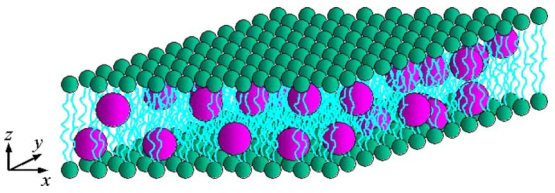

FIG. 1. (Color online) A schematic of the lipid bilayer membrane containing inclusions. The small solvent molecules on the two sides of the membrane are not plotted here.

count reasonably well for lateral inhomogeneity of the lipid bilayers, although less molecular details are considered. Here we put emphasis on the description of laterally heterogeneous structures of lipid membranes with the presence of nanoparticles, where the molecular details of lipids are not important.

In this paper, we will study the variation in lateral structure of membrane with the increase in inclusions. Our aim is to discover the main factors affecting the organization of inclusions within membranes, as well as the structure of perturbed membranes compared with the experimental observations. It should be mentioned that lipid membranes are made up of amphiphilic molecules, which are assumed to be in the liquid phase at a relative high temperature. Therefore, lipid tails are much more flexible than inclusions. It is more reasonable to use the hybrid SCFT/DFT approach [30] to calculate the structural organization of the bilayer membrane in the presence of inclusions. The present paper is organized as follows. First, we describe the hybrid SCFT/DFT theory for lipid-inclusion complexes. Then, we present relevant results and explore main factors determining the structure of inclusion-containing membranes. In the last section, we draw conclusions on nanosized hydrophobic particles embedded in lipid bilayers and discuss how to extend our model to other membrane systems.

II. METHODS

We consider a lipid bilayer membrane containing n_d inclusions of radius R in an aqueous environment (Fig. 1). The volume of system is $V=L_x\times L_y\times L_z$, where L_x and L_y are lateral membrane lengths under periodical boundary conditions, and L_z is the size of the system along the membrane normal direction. The bilayer membrane is composed of one type of lipid with two hydrophobic tails. The number of lipids is given by $n_l=2\times\sigma\times L_x\times L_y$, where σ is the number density of lipids in one leaflet. The head group of lipids has the volume v_h, and two equal-length tails composed of $N/2$ segments each are assumed as flexible Gaussian chains [40], which is reasonable for the description of lipid membranes in liquid phase. Therefore, N is the total segment number of two tails forming a lipid. The segment has the volume ρ_0^{-1} and the length a. The concentrations of the head and tails of lipids are $\phi_h=n_l v_h/V$ and $\phi_t=n_l N\rho_0^{-1}/V$, and the inclusions $\phi_d=4\pi R^3 n_d/3V$. The solvent molecules have the volume v_s and the concentration ϕ_s. Since many bioinclusions are effectively smooth and rigid compared to the lipid tails [1,8,25], we assume inclusions as hard-sphere nanoparticles.

In the framework of SCFT, we first transform a Hamiltonian of the lipid system into a coarse-grained field theory description by employing the simple Gaussian model for lipid chains [40] and treating their interactions through mean-field Flory-Huggins form. Further, by combining the steric interactions between inclusions through DFT [30], the resulting free energy F for the present system is given by

$$\begin{aligned}\frac{NF}{\rho_0 k_B TV} =& -\phi_t \ln\left(\frac{Q_l}{V\phi_t}\right)-\frac{\phi_s}{\alpha_s}\ln\left(\frac{Q_s}{V\phi_s}\right)-\frac{\phi_d}{\alpha}\ln\left(\frac{Q_d\alpha}{V\phi_d}\right)\\ &+\frac{1}{V}\int d\mathbf{r}\{\chi_{th}N\varphi_t(\mathbf{r})\varphi_h(\mathbf{r})+\chi_{ts}N\varphi_t(\mathbf{r})\varphi_s(\mathbf{r})\\ &+\chi_{td}N\varphi_t(\mathbf{r})\varphi_d(\mathbf{r})+\chi_{hs}N\varphi_h(\mathbf{r})\varphi_s(\mathbf{r})\\ &+\chi_{hd}N\varphi_h(\mathbf{r})\varphi_d(\mathbf{r})+\chi_{sd}N\varphi_s(\mathbf{r})\varphi_d(\mathbf{r})-w_t(\mathbf{r})\varphi_t(\mathbf{r})\\ &-w_h(\mathbf{r})\varphi_h(\mathbf{r})-w_s(\mathbf{r})\varphi_s(\mathbf{r})-w_d(\mathbf{r})\rho_d(\mathbf{r})-\xi(\mathbf{r})[1\\ &-\varphi_t(\mathbf{r})-\varphi_h(\mathbf{r})-\varphi_s(\mathbf{r})-\varphi_d(\mathbf{r})]+\rho_d(\mathbf{r})\Psi_{hs}(\bar{\varphi}_d)\},\end{aligned} \tag{1}$$

where k_B is the Boltzmann constant and T is the temperature. The first three terms in the free energy, Eq. (1), account for the entropy part of the system. Q_l, Q_s, and Q_d are single molecular partition functions of lipid, solvent, and nanoparticle, respectively. The expression of Q_l is given by $Q_l=\int d\mathbf{r}q_l(\mathbf{r},s)q_l(\mathbf{r},1-s)$, where s ranges from 0 at the end of one tail to $s=1$ the end of the other tail. The end-segment distribution function $q_l(\mathbf{r},s)$ satisfies modified diffusion equation $\frac{\partial q_l}{\partial s}=\frac{a^2N}{6}\nabla^2 q_l-[\alpha_h w_h(\mathbf{r})\delta(s-1/2)+w_t(\mathbf{r})]q_l$, where $s=1/2$ is the location of the head, and the volume ratio of a head to two tails of the lipid is $\alpha_h\equiv v_h\rho_0/N$. The initial condition of the modified diffusion equation is $q_l(x,y,z,0)=1$. The partition function of a solvent is $Q_s=\int d\mathbf{r}\exp[-\alpha_s w_s(\mathbf{r})]$, where the volume ratio of a solvent molecule to two tails of a lipid is $\alpha_s\equiv v_s\rho_0/N$. The partition function of a particle is $Q_d=\int d\mathbf{r}\exp[-w_d(\mathbf{r})]$ and the volume ratio of a particle to two tails is $\alpha\equiv 4\pi R^3\rho_0/3N$. $\varphi_t(\mathbf{r})$, $\varphi_h(\mathbf{r})$, $\varphi_d(\mathbf{r})$, and $\varphi_s(\mathbf{r})$ are the local volume fractions of lipid tail, head group, inclusion, and solvent. The effective interactions between different species are represented by the Flory parameters; i.e., χ_{th}, χ_{ts}, χ_{td}, χ_{hs}, χ_{hd}, and χ_{sd} account for the local interactions between tail-head, tail-solvent, tail-inclusion, head-solvent, head-inclusion, and solvent-inclusion, respectively. In the self-consistent field theory, intermolecular interactions are simplified as effective fields felt by different molecules, which are reflected by $w_t(\mathbf{r})$, $w_h(\mathbf{r})$, $w_d(\mathbf{r})$, and $w_s(\mathbf{r})$ with the corresponding energetic terms like $\varphi_i(\mathbf{r})w_i(\mathbf{r})(i=t,h,d,s)$ in Eq. (1). The packing constraint of the system is realized by an incompressible constraint: $\varphi_t+\varphi_h+\varphi_s+\varphi_d=1$; it is reported that such a substitution is reasonable and computational efficient [13,40,44], while the exact packing interaction between different compositions can been done by density-functional theory for polymer-colloid mixtures [45,46]. $\xi(\mathbf{r})$ is a Lagrange multiple, which induces the incompressible constraint into the free energy. The last term in Eq. (1) is the nonideal steric repulsion between the hard particles, in which $\Psi_{hs}(x)=\frac{4x-3x^2}{(1-x)^2}$ [38,39], with the weighted inclusion density $\bar{\varphi}_d(\mathbf{r})$ [30]. $\rho_d(\mathbf{r})$ stands for the

inclusion center distribution and the local volume fraction φ_d is given by $\varphi_d(\mathbf{r})=\frac{3\alpha}{4\pi R^3}\int_{|\mathbf{r}'|<R}d\mathbf{r}'\rho_d(\mathbf{r}+\mathbf{r}')$.

By minimizing the free energy in Eq. (1), we obtain a set of self-consistent equations describing the equilibrium system:

$$\varphi_t(\mathbf{r}) = \frac{\phi_t V}{Q_l}\int_0^1 ds q_l(\mathbf{r},s)q_l(\mathbf{r},1-s), \tag{2}$$

$$\varphi_h(\mathbf{r}) = \frac{\phi_h V}{Q_l}\exp[-\alpha_h W_h(\mathbf{r})]q_l\left(\mathbf{r},\frac{1}{2}\right)q_l\left(\mathbf{r},\frac{1}{2}\right), \tag{3}$$

$$\varphi_s(\mathbf{r}) = \frac{\phi_s V}{Q_s}\exp(-\alpha_s W_s), \tag{4}$$

$$\rho_d(\mathbf{r}) = \frac{\phi_d V}{\alpha Q_d}\exp[-W_d(\mathbf{r})], \tag{5}$$

$$W_t(\mathbf{r}) = \chi_{th}N\varphi_h + \chi_{ts}N\varphi_s + \chi_{td}N\varphi_d + \xi(\mathbf{r}), \tag{6}$$

$$W_h(\mathbf{r}) = \chi_{th}N\varphi_t + \chi_{hs}N\varphi_s + \chi_{hd}N\varphi_d + \xi(\mathbf{r}), \tag{7}$$

$$W_s(\mathbf{r}) = \chi_{ts}N\varphi_t + \chi_{hs}N\varphi_h + \chi_{sd}N\varphi_d + \xi(\mathbf{r}), \tag{8}$$

$$\begin{aligned} W_d(\mathbf{r}) = {} & \Psi_{hs}[\bar{\varphi}_d(\mathbf{r})] + \frac{\alpha}{v_R}\int_{|r'|<R} d\mathbf{r}'[\chi_{td}N\varphi_t(\mathbf{r}+\mathbf{r}') \\ & + \chi_{hd}N\varphi_h(\mathbf{r}+\mathbf{r}') + \chi_{sd}N\varphi_s(\mathbf{r}+\mathbf{r}') + \xi(\mathbf{r}+\mathbf{r}')] \\ & + \frac{\alpha}{v_{2R}}\int_{|r'|<2R} d\mathbf{r}'\{\rho_d(\mathbf{r}+\mathbf{r}')\Psi'_{hs}[\bar{\varphi}_d(\mathbf{r}+\mathbf{r}')]\}. \end{aligned} \tag{9}$$

Here the volume fractions and fields of different components are coupled, which are solved self-consistently. Using the real space combinatorial screening algorithm [32], we perform calculations starting from the random initial conditions of densities. In each calculation, once densities of different compositions are determined, fields can be calculated. The densities are then updated from the calculated fields and new fields are recalculated. This step is repeated until the packing constraints are satisfied. The given results are selected to have the minimum free energy among different initial conditions. Furthermore, free-energy minimization of the system with respect to the selected simulation sizes is also performed [37].

According to the free-energy expression (1), we can obtain some useful quantities. First, the translational entropy S_d of inclusions can be given by

$$\frac{NS_d}{k_B\rho_0 V} = \frac{\phi_d}{\alpha}\ln\left(\frac{Q_d\alpha}{V\phi_d}\right) + \frac{1}{V}\int d\mathbf{r}[w_d(\mathbf{r})\rho_d(\mathbf{r})]. \tag{10}$$

It can be obtained from the free energy of inclusions exempted by enthalpy part due to the interactions between inclusions and other species. Second, the translational entropy S_{tr} of lipids is written as

$$\frac{NS_{tr}}{k_B\rho_0 V} = -\frac{1}{V}\int d\mathbf{r}\rho(\mathbf{r})\ln[\rho(\mathbf{r})]. \tag{11}$$

Since a lipid includes many segments, here we choose the motion of the middle point of a lipid tail as the translational movement of the lipid. $\rho(\mathbf{r})$ is the density of the middle point of a lipid tail, i.e., $\rho(\mathbf{r})=\frac{\phi_t V}{Q_l}q_l(\mathbf{r},\frac{1}{4})q_l(\mathbf{r},\frac{3}{4})$. Third, the conformational entropy S_c of lipids is expressed as

$$\frac{NS_c}{k_B\rho_0 V} = \frac{1}{V}\int d\mathbf{r}\left\{\rho(\mathbf{r})\ln\left[q_l\left(\mathbf{r},\frac{1}{4}\right)q_l\left(\mathbf{r},\frac{3}{4}\right)\right] + w_t(\mathbf{r})\varphi_t(\mathbf{r})\right\}, \tag{12}$$

which comes from the total entropy of lipids exempted by the translational entropy, that is, the movements of total segments except for the middle point of the tail. Finally, the steric repulsion energy F_{st} of inclusions is

$$F_{st} = \int d\mathbf{r}\rho_d(\mathbf{r})\Psi_{hs}(\bar{\varphi}_d). \tag{13}$$

This is the nonideal term because of the steric repulsion arising from the hard particles.

In our model, Flory parameters are used to describe the effective interactions between different components instead of the real interactions. At this point, the relative values of Flory parameters become more significant. The principle of choosing Flory parameters is to ensure that nanoparticles are embedded within the lipid membrane, while the solvents are out of the hydrophobic region of the membrane. We choose $\chi_{hs}N=0$, which is taken as a reference, implying that there is no repulsive interaction between head group and solvent. $\chi_{ts}N$ is fixed as 15.0 accounting for the hydrophobic interaction between tails of the lipid and solvent. $\chi_{th}N$ is equal to 25.0, reflecting the chemical bond between head and tail parts of the lipid. Values of $\chi_{sd}N$, $\chi_{hd}N$, and $\chi_{td}N$ are chosen as 20.0, 15.0, and 3.5, respectively, meaning that the particles are hydrophobic. We fix all the Flory parameters in the following calculations because we pay more attention to the effect of the concentration of inclusions on the lateral structure of the membrane. Other parameters used in our calculations are fixed as $N=32$, $v_h=v_s=6\rho_0^{-1}$, and $\sigma=0.08$. The system size is selected to be $L_x=L_y=60a$ and $L_z=15a$. Here, the chosen L_z is large enough, ensuring the solvent concentration $\phi_s=1$ at $z=0$ and L_z. The inclusion size is chosen as $R=2.5a$, which is a little bit smaller than the thickness of the unperturbed membrane.

III. RESULTS AND DISCUSSIONS

We first examine the case of a bilayer membrane in an aqueous environment in the absence of inclusions. Figure 2(a) shows the lateral distribution of lipid tails in one leaflet, which is uniform. The distribution is symmetrical with respect to the opposing leaflet. Figure 2(b) provides the average distribution of head groups in the x-z cross sections, reflecting that the shape of membrane surfaces is smooth in the absence of inclusions, where the membrane is unperturbed. In this case, the membrane has the limited lateral

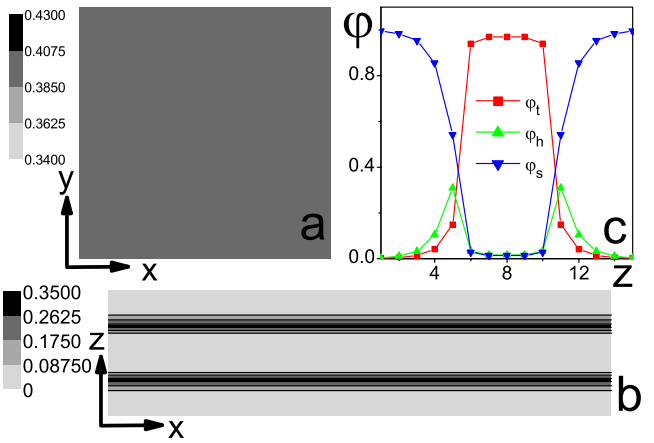

FIG. 2. (Color online) The pure bilayer membrane in an aqueous environment. (a) The top view of averaged density distribution of lipid tails in the upper leaflet. (b) The x-z cross section of density distribution of lipid heads averaged in the y direction. (c) Laterally averaged density profiles of solvent (φ_s), lipid tail (φ_t), and head group (φ_h) along z axes.

mobility [20], where lipid tails crossly interact and tightly pack. Figure 2(c) shows the laterally averaged density profiles of φ_t, φ_h, and φ_s across a bilayer, which displays the basic structure of the bilayer and is favorably comparable with mesoscopic simulation and other coarse-grained models describing the bilayer composition [41,47,48]. This validates the used SCFT which can reasonably explore conformational properties of lipids, in contrast to phenomenological models that ignore much of the internal structure of the bilayer [24]. Particularly, the approach will become powerful in exploring the lateral inhomogeneity of membrane with inclusions, in contrast to other field theory or simulation schemes [24], where the only one-dimensional density profiles along the membrane normal are shown.

Figure 3 shows the in-plane density distributions of inclusions in the left column and the lipid tails in the right column with increasing the inclusion concentration ϕ_d. When the concentration ϕ_d of inclusions is low, the translational entropy of inclusions has a significant contribution to the free energy of the system. Any compositional fluctuation of inclusions may lead to the lateral inhomogeneity of lipid composition, in which lipids are depleted in the inclusion-rich regions for ensuring the large translational entropy of inclusions [Fig. 3(a)]. Astonishingly, as ϕ_d is increased, not only the aggregation of inclusions is strengthened, but also the lipid/inclusion-rich domains appear [Fig. 3(b)]. This is because the inclusions incline to aggregate into clusters for decreasing enthalpy due to the positive χ_{td}, while lipids tend to accumulate around inclusions. In this case, the entropic contribution of lipids becomes significant. Usually, in the pure membrane, lipids interact crossly and pack tightly, while a single lipid can easily change its conformation. As hard inclusions are added into the membrane, the tight packing of lipids is disturbed. Lipid tails closing to the rigid surfaces of inclusions can get extra conformational flexibility [1,23,28,29,49], which drives them gathering around the inclusions, and thus lipid-rich microdomains are formed. The domain size may be enlarged by increasing ϕ_d [Fig. 3(c)]

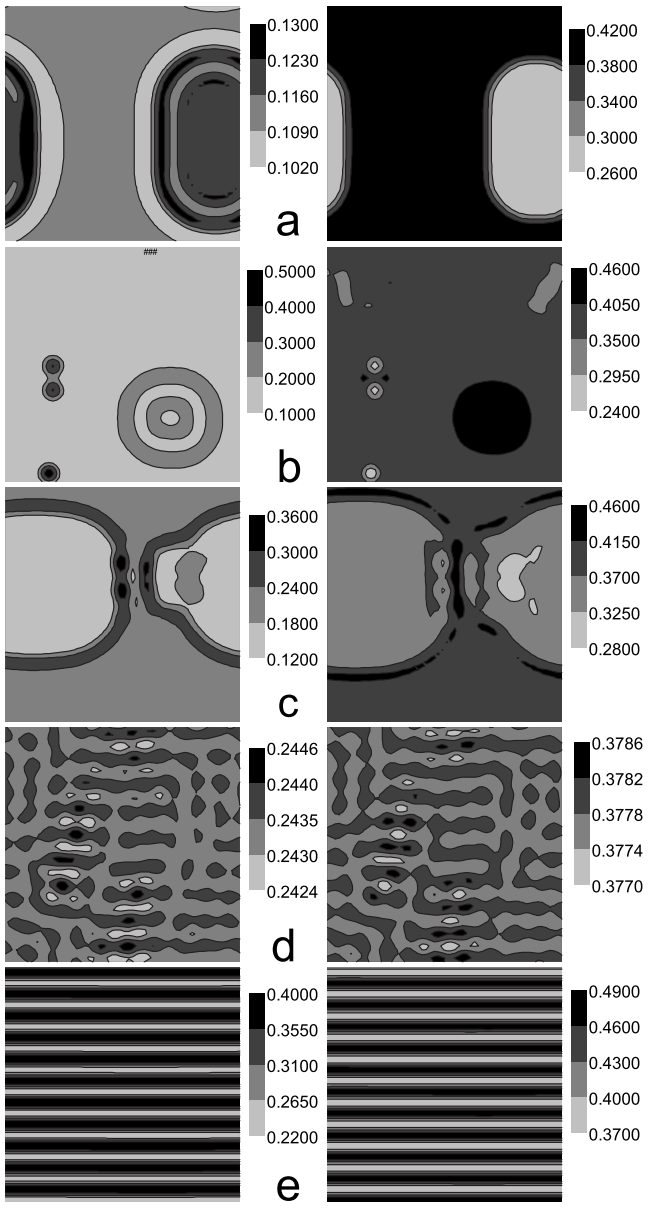

FIG. 3. The top views of averaged density distributions of inclusions (left) and lipid tails (right) in upper leaflet. (a) ϕ_d=0.10, (b) ϕ_d=0.15, (c) ϕ_d=0.20, (d) ϕ_d=0.24, and (e) ϕ_d=0.32. Here we fix R=2.5a which is smaller than the membrane thickness.

because the steric repulsions between hard inclusions begin to play a role. At the same time, the aggregation of inclusions is weakened. Interestingly, as ϕ_d is added to a certain range (ϕ_d=0.24–0.28), lipid-rich domains disappear, but instead the almost uniform distribution of both inclusion and lipid tail occurs [Fig. 3(d)]. This unexpected behavior provides a strong support for the experimental findings in drug-membrane [15] and cholesterol-membrane [18] complexes. The reason is that the strong steric repulsions lead to the uniform distribution of the inclusions, which, in turn, causes the homogeneous distribution of lipids. Moreover, lipid tails undergo the confinement from the surrounding inclusions due to the high concentration of inclusions. With further increase in ϕ_d, the release of deformed conformational entropy of lipids induces lipid-mediated depletion attraction, leading

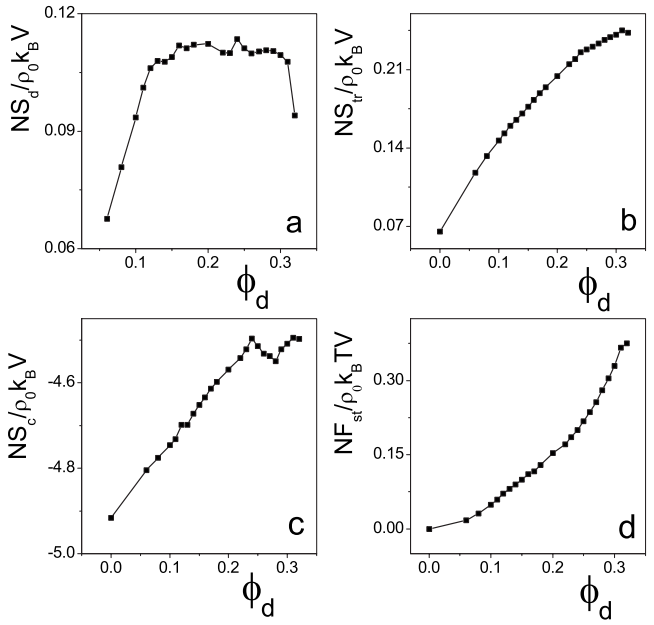

FIG. 4. (a) The translational entropy S_d of inclusions, (b) the translational entropy S_{tr} of lipids, (c) the conformational entropy S_c of lipids, and (d) the steric energy F_{st} of inclusions vs the inclusion concentration.

to the chaining arrangement of inclusions shown in Fig. 3(e). Such a regularly modulated inclusion-rich stripe structure has been reported in the drug-membrane [15,20] and cholesterol-membrane complexes [18,19] where the lipids form ribbons between the aligned cholesterol domains.

As is mentioned above, the structures in Fig. 3 correspond to the minimization of free energy for different initial conditions, although the difference of free energy with different random seeds is small. It is found that the asymmetric structures in Figs. 3(a)–3(c) depend on different initial perturbation conditions. For instance, the position and size of the lipid/inclusion-rich domains in Fig. 3(b) change with varying the initial conditions. However, the main characters of the structure remain unchanged.

To understand the physical mechanisms underlying the above phenomena, we focus on several important quantities controlling the structural change in the membrane. With increasing the concentration of inclusions, we find that the total free energy of the system increases continuously. Instead, the entropies of lipids and inclusion and the steric repulsion between inclusions display significant changes, which play important roles on the structure change of inclusion-containing membranes. Therefore, we will study the entropy and repulsive energy contributions separately to disclose their different roles on the structure transition. Figure 4(a) shows the variation in translational entropy S_d of inclusions with the increasing concentration of inclusions. For low ϕ_d, the large increase in S_d with ϕ_d indicates that S_d plays an important role at first, which can account well for the formation of the weak inhomogeneous distribution of lipids [Fig. 3(a)] to ensure large translational entropy of inclusions. For large ϕ_d, S_d decreases with the appearance of the chaining structure. Figure 4(b) shows the translational entropy S_{tr} of lipids as a function of the inclusion concentration. The curve of translational entropy of lipids goes up monotonously, meaning that the addition of inclusions increases the lateral movement of lipids in the membrane. Experiments have found that the lateral membrane fluidity [18,20] increases with the addition of inclusions of membrane. Here, the increase in the translational entropy S_{tr} of lipids reveals the increase in the translational degree of freedom of lipids, while it does not sign the fluidity of the membrane directly. In the present case, the addition of inclusions breaks the cross interaction between lipid tails, which inhibits the tight packing of the pure membrane, and thus increases the possibility of the lateral movement of lipids [1]. Figure 4(c) shows the conformational entropy S_c of lipids as a function of the inclusion concentration. Beginning from a low conformational entropy of the pure membrane, lipids get more conformations around the hard inclusions, where the lipid-enriched rafts are formed. However, there is a decrease in the range ϕ_d=0.24–0.28 with the disappearance of lipid rafts, where lipids chains are confined due to the surrounding inclusions. Figure 4(d) shows the steric repulsion energy F_{st} of inclusions, which increases with increasing the inclusion concentration ϕ_d. Such repulsions tend to cause the uniform distribution of inclusions. For high ϕ_d, the repulsion of inclusions is stronger, but at the same time, the deformed lipid-mediated attraction between inclusions becomes also stronger. The only way that the conformational entropy of deformed lipids is released [Fig. 4(c)] is to drive inclusions to assemble anisotropically along one direction. As a result, the deformed lipids provide an additional lateral anisotropic depletion interaction between inclusions, which stabilizes the parallel chain arrays of inclusions.

Figure 5 shows laterally averaged density profiles of different components across the bilayer in the left column and average density distributions of lipid heads in x-z cross sections in the right column. For low concentration ϕ_d of inclusions [Fig. 5(a)], the inclusions assemble in the bilayer midplane for the membrane stability, which is displayed by one peak of density profiles (φ_d) of inclusions. With increasing ϕ_d, one peak density profile may be saturated [Fig. 5(b)] and further increase in inclusions leads to the occurrence of two peaks of φ_d [Figs. 5(c)–5(e)], implying the relocation of inclusions where the two-layer distribution of inclusions is arranged in opposing leaflets of a bilayer [49]. Previous experiment [20] on drug-membrane complexes has also shown that the location of drugs in the bilayer depends on drug content. The two-layer distribution of inclusions ensures that the ends of lipid tails can still remain in the membrane midplane favoring the conformation of lipids. On the other hand, in Figs. 5(a)–5(c), the irregular density distribution of head groups originates from the lipid chain-length mismatch, while in Fig. 5(d), the membrane surfaces become flat with a matched length of confined lipids where lipid-rich domains disappear and the uniform distribution of lipids and inclusions occurs. By comparison of the distances between two peaks of head profiles (φ_h) in the left side of Fig. 5, we also find that the thickness of membrane continuously increases with the addition of inclusions. Finally, Fig. 6 provides a schematic of the morphological change in the system. In the pure membrane case [Fig. 6(a)], lipids interact crossly and pack tightly. With the addition of inclusions, the distribution of lipids is

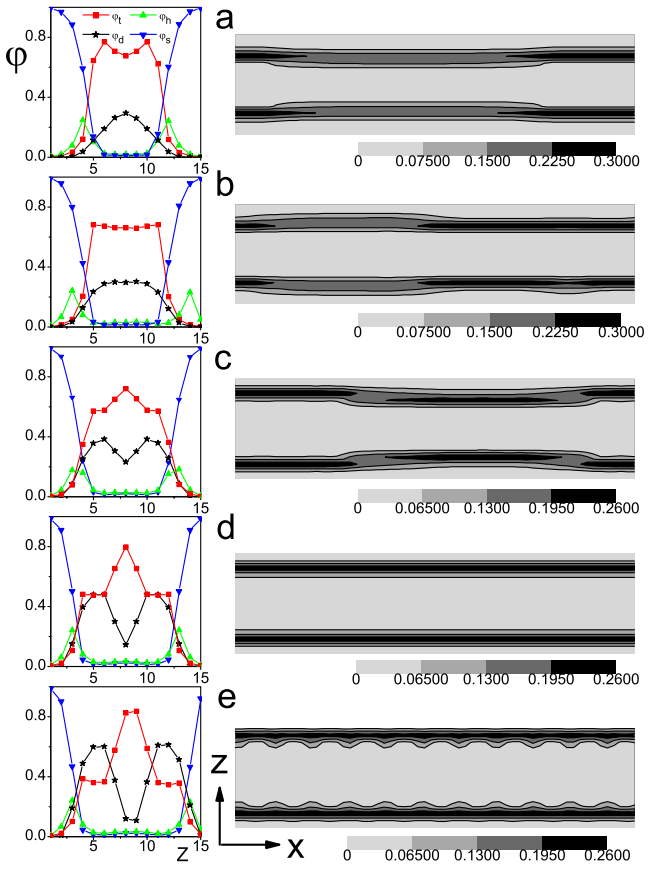

FIG. 5. (Color online) Laterally averaged density profiles of solvent (φ_s), lipid tail (φ_t), head group (φ_h), and inclusion (φ_d) along z axes (left), and the x-z cross sections of density distributions of lipid heads averaged in the y direction (right). Parameters are the same in Fig. 3.

perturbed as shown in Figs. 6(b)–6(f). The cross-link between lipids becomes less and less with increasing the concentration of inclusions and the thickness of the membrane becomes larger and larger, which is good for the increase in both the translational and conformational entropies of lipids. Furthermore, the distribution of inclusions changes from one layer to two layers.

IV. CONCLUSIONS

In summary, the present study advances our understanding of membrane organization by unifying these experimental evidences of the realistic biomembranes in the presence of different inclusions. The results can account well for a series of unexpected behaviors in related experimental findings. (1) The appearance and disappearance of inclusion/lipid-rich domains are observed with increasing inclusions. (2) Location of inclusions changes with increasing inclusions

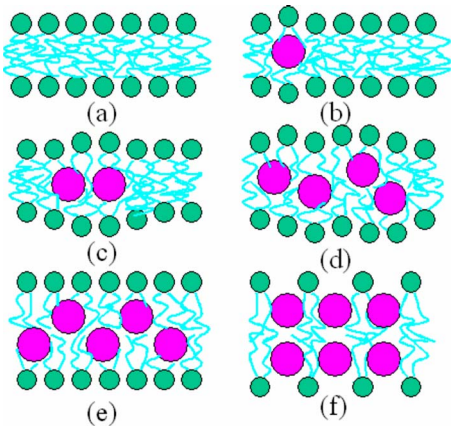

FIG. 6. (Color online) A schematic figure of a sideways cut through the bilayer illustrating the morphological change in the system with the increase in the inclusions, where the locations of the inclusions and lipids (heads and tails) are clearly marked.

and may undergo a layering transition from one-layer structure located in the center of the bilayer to two-layer structure arranged in opposing leaflets of a bilayer. (3) The chain arrays of inclusions may form at high inclusion content. (4) The lateral movement of lipids is enhanced by the presence of inclusions. Here, the deformed lipid chains regulate the lateral interactions between the lipids and inclusions to organize the composition segregation of inclusion-membrane complexes. We suggest that the competition between the conformational entropy of lipids and the steric repulsion of inclusions plays a very important role in determining the organization of lipid bilayers at the presence of inclusions.

The lateral structure of lipid membranes with inclusions largely depends on the size and shape of inclusions, as well as the nature of lipid molecules. Here we only consider a simple model, in which inclusions are small hydrophobic nanoparticles and lipid tails are completely flexible. However in real biological systems, the size of many inclusions is larger than the thickness of membrane, and they are composed of both hydrophobic and hydrophilic parts such as protein and cholesterol. Thus, models for inclusions become much more complicated. Furthermore, recent works show that lipid membranes undergo the liquid-gel transition with the decrease in temperature or with the increase in inclusions. To account for the liquid-gel transition, the Gaussian model for lipid tails needs to be improved. These will be two main challenges in the field of membrane/inclusion systems for the further works.

ACKNOWLEDGMENTS

This work was supported by the National Basic Research Program of China under Grant No. 2007CB925101 and the National Natural Science Foundation of China under Grants No. 10804045, No. 10629401, and No. 20674037.

[1] O. G. Mouritsen, *Life—As a Matter of Fat* (Springer-Verlag, Berlin, 2005).
[2] L. Miao, M. Nielsen, J. Thewalt, J. H. Ipsen, M. Bloom, M. J. Zuckermann, and O. G. Mouritsen, Biophys. J. **82**, 1429 (2002).
[3] F. Maxfield and I. Tabas, Nature (London) **438**, 612 (2005).
[4] K. Simons and W. Vaz, Annu. Rev. Biophys. Biomol. Struct. **33**, 269 (2004).
[5] H. McConnell and M. Vrljic, Annu. Rev. Biophys. Biomol. Struct. **32**, 469 (2003).
[6] M. Edidin, Annu. Rev. Biophys. Biomol. Struct. **32**, 257 (2003).
[7] D. Brown and E. London, Annu. Rev. Cell Dev. Biol. **14**, 111 (1998).
[8] H. Ohvo-Rekila, B. Ramstedt, P. Leppimaki, and J. P. Slotte, Prog. Lipid Res. **41**, 66 (2002).
[9] K. Simons and E. Ikonen, Science **290**, 1721 (2000).
[10] T. Baumgart, S. Hess, and W. Webb, Nature (London) **425**, 821 (2003).
[11] S. Komura and D. Andelman, Europhys. Lett. **64**, 844 (2003).
[12] H. McConnell and A. Radhakrishnan, Proc. Natl. Acad. Sci. U.S.A. **103**, 1184 (2006).
[13] R. Elliott, I. Szleifer, and M. Schick, Phys. Rev. Lett. **96**, 098101 (2006).
[14] S. L. Veatch and S. L. Keller, Phys. Rev. Lett. **94**, 148101 (2005).
[15] S. Feng, K. Gong, and J. Chew, Langmuir **18**, 4061 (2002).
[16] C. Bernsdorff, R. Reszka, and R. J. Winter, J. Biomed. Mater. Res. **46**, 141 (1999).
[17] P. Nassar, L. Almeida, and M. Tabak, Biochim. Biophys. Acta **1328**, 140 (1997); Langmuir **14**, 6811 (1998).
[18] J. C. Lawrence, D. E. Saslowsky, J. M. Edwardson, and R. M. Henderson, Biophys. J. **84**, 1827 (2003).
[19] J. Rogers, A. G. Lee, and D. D. Wilton, Biochim. Biophys. Acta **552**, 23 (1979).
[20] S. V. Balasubramanian and R. M. Straubinger, Biochemistry **33**, 8941 (1994).
[21] A. Zemel, A. Ben-Shaul, and S. May, Biophys. J. **86**, 3607 (2004).
[22] S. May and A. Ben-Shaul, Phys. Chem. Chem. Phys. **2**, 4494 (2000).
[23] S. H. Park, S. G. Oh, J. Y. Mun, and S. S. Han, Colloids Surf. B Biointerfaces **44**, 117 (2005).
[24] M. Müller, K. Katsov, and M. Schick, Phys. Rep. **434**, 113 (2006) and references therein. This review has justified the recent applications of coarse-grained SCFT with Gaussian chain model to bilayer membrane.
[25] M. Venturoli, M. Sperotto, M. Kranenburg, and B. Smit, Phys. Rep. **437**, 1 (2006).
[26] M. Sperotto, S. May, and A. Baumgaertner, Chem. Phys. Lipids **141**, 2 (2006).
[27] N. Dan, P. Pincus, and S. Safran, Langmuir **9**, 2768 (1993).
[28] R. Bruinsma and P. Pincus, Curr. Opin. Solid State Mater. Sci. **1**, 401 (1996).
[29] S. May, Langmuir **18**, 6356 (2002).
[30] R. B. Thompson *et al.*, Science **292**, 2469 (2001); Macromolecules **35**, 1060 (2002).
[31] M. W. Matsen and M. Schick, Phys. Rev. Lett. **72**, 2660 (1994).
[32] F. Drolet and G. H. Fredrickson, Phys. Rev. Lett. **83**, 4317 (1999).
[33] C. L. Ren and Y. Q. Ma, J. Am. Chem. Soc. **128**, 2733 (2006).
[34] F. Schmid, J. Phys.: Condens. Matter **10**, 8105 (1998).
[35] G. H. Fredrickson, *The Equilibrium Theory of Inhomogeneous Polymers* (Oxford University Press, Oxford, 2006).
[36] M. W. Matsen, in *Soft Matter*, edited by G. Gompper and M. Schick (Wiley-VCH, Weinheim, 2006), Vol. 1.
[37] Y. Bohbot-Raviv and Z. G. Wang, Phys. Rev. Lett. **85**, 3428 (2000).
[38] P. Tarazona, Mol. Phys. **52**, 81 (1984).
[39] N. F. Carnahan and K. E. Starling, J. Chem. Phys. **51**, 635 (1969).
[40] X. J. Li and M. Schick, Biophys. J. **78**, 34 (2000) compares the SCFT results of the lipid system with the experimental results, and a good agreement is found between them, while the real lipid is not completely flexible.
[41] R. A. Kik, F. A. M. Leermakers, and J. M. Kleijn, Phys. Chem. Chem. Phys. **7**, 1996 (2005).
[42] L. A. Meijer, F. A. M. Leermakers, and J. Lyklema, J. Chem. Phys. **110**, 6560 (1999).
[43] F. A. M. Leermakers, A. L. Rabinovich, and N. K. Balabaev, Phys. Rev. E **67**, 011910 (2003).
[44] R. Elliott, K. Katsov, M. Schick, and I. Szleifer, J. Chem. Phys. **122**, 044904 (2005).
[45] D. Cao and J. Wu, J. Chem. Phys. **126**, 144912 (2007).
[46] E. S. McGarrity, A. L. Frischknecht, L. J. D. Frink, and M. E. Mackay, Phys. Rev. Lett. **99**, 238302 (2007).
[47] A. L. Frischknecht and Laura J. Douglas Frink, Phys. Rev. E **72**, 041924 (2005).
[48] J. C. Shillcock and R. Lipowsky, J. Chem. Phys. **117**, 5048 (2002).
[49] M. B. Sankaram and T. E. Thompson, Biochemistry **29**, 10676 (1990).